Published in final edited form as:
Nat Struct Mol Biol. 2010 February ; 17(2): 144–150. doi:10.1038/nsmb.1736.

Allosteric regulation of Argonaute proteins by miRNAs

Sergej Djuranovic[*,1], **Michelle Kim Zinchenko**[*,1], **Junho K. Hur**[1], **Ali Nahvi**[1], **Julie L. Brunelle**[1], **Elizabeth J. Rogers**[1], and **Rachel Green**[1]

[1]Howard Hughes Medical Institute and Department of Molecular Biology and Genetics, Johns Hopkins University School of Medicine, Baltimore, MD 21205, USA.

Abstract

Small interfering RNAs (siRNAs) and microRNAs (miRNAs) bind to Argonaute family proteins to form a related set of effector complexes that play diverse roles in post-transcriptional gene regulation throughout the eukaryotic lineage. Here, sequence and structural analysis of the MID domain of the Argonaute proteins identified similarities with a family of allosterically regulated bacterial ligand-binding domains. *In vitro* and *in vivo* approaches were used to show that certain Argonaute proteins (those involved in translational repression) have conserved this functional allostery between two distinct sites, one involved in binding miRNA:target duplex and the other in binding the 5' cap feature (m^7GpppG) of eukaryotic mRNAs. This allostery provides an explanation for how miRNA-bound effector complexes may avoid indiscriminate repressive action (mediated through binding interactions with the cap) prior to full target recognition.

Keywords

Argonaute; miRNA; miRNP; m^7GpppG cap; allostery

Small interfering RNAs (siRNAs) and microRNAs (miRNAs) belong to an increasingly broad class of small, non-coding RNA molecules found in diverse organisms[1]. These two groups are broadly distinguished by their biogenesis pathways and their differential loading into distinct Argonaute complexes. siRNAs are generated in the cytoplasm and are loaded into an Argonaute-containing RNA-induced silencing complex (siRISC) to cleave targets with perfect complementarity. miRNAs are transcribed in the nucleus from a specific gene and are ultimately loaded into Argonaute-containing miRNPs (miRISC) that limit the expression of distinct mRNA targets with imperfect complementarity. And, though there are clearly shared molecular features for these two processes (*e.g.* an Argonaute protein and a small RNA), there are also distinct molecular features and players important both for small RNA loading and target recognition[2]. The Argonaute proteins are composed of several distinct domains with partially understood functions: an N-terminal domain, a PAZ domain that contains the binding site for the 3' end of the small RNA, a MID domain that contains the binding site for the 5' end of the small RNA (which will be the focus of discussion in this manuscript), and the PIWI domain that contains the catalytic center for the cleavage reaction that occurs during RNA interference (Fig. 1a).

A number of molecular mechanisms have been proposed to account for the observed post-transcriptional control of miRNA-targeted genes including inhibition of translation initiation or elongation and the promotion of mRNA decay (reviewed in ref. 3). One previous study

Correspondence should be addressed to R.G. (ragreen@jhmi.edu)..
*These authors contributed equally to this work.

Author Information The authors declare no competing financial interests.

identified potential sequence similarities between the MID domain of the Argonaute protein family and the m^7GpppG (cap) binding domain of the eukaryotic translation initiation factor eIF4E[4], immediately suggesting models of regulation directly targeting the cap-dependent step of translation initiation; indeed a number of studies have reported connections between the cap and translational repression[5-10]. However, studies by a number of other laboratories have questioned the relevance of this observed cap binding, and have argued instead that GW182 recruitment by the Argonaute protein is sufficient to explain miRNA-mediated repression[11-13]. Here we use purified proteins from various species as well as an *in vivo Drosophila* system to provide evidence for allostery in the Argonautes that coordinates the binding of miRNAs, cap, and potentially other ligands, to promote miRNA-mediated translational repression in these systems.

RESULTS

Argonaute MID domain analysis reveals functional groupings

The mechanistic questions that arose from the studies by Mourelatos and colleagues prompted us to perform more extensive bioinformatic analyses on the Argonaute family of proteins. Sequence similarity searches with the MID domains from the *Drosophila* Argonautes DmAgo1 and DmAgo2 returned only known members of the Argonaute/PIWI protein family as matches with BLAST and PSI-BLAST, yet no eIF4E family members. Moreover, full alignments that included eukaryal, archaeal and bacterial homologs of the MID domain showed that phenylalanine residues proposed to be important for cap binding[4] were not universally conserved (Supplementary Fig. 1). We next used HHpred[14] to identify more remote homologs of the chosen protein, and were able to identify the ligand-binding domains from a large class of bacterial proteins including the *PurR* and *LacI* transcription factors. We see that these bacterial ligand-binding domains share high structural similarity with the known structures of the Argonaute MID domains (Fig. 1b), as previously noted by others[15]. Importantly, the structure of eIF4E[16] shares no similarity with the known structure of the Argonaute MID domain (Fig. 1c). Based on alignment of the DmAgo1-MID domain sequence with known Argonaute MID domain structures, we created a model for use in a DALI structure-based search[17]. These searches confirmed the observed sequence similarity (above) with the *PurR/LacI* transcription factors and led to the inclusion of numerous other proteins (Supplementary Fig. 2a-c). These proteins all share a common Rossmann-like fold, and many exhibit allosteric behavior wherein binding of metabolites (for example, nucleotides) in one site is coupled to functional interactions in an independent site[18].

We next used a clustering analysis of 834 Argonaute/PIWI sequences using a JAVA program, CLANS[19], which clusters the distinct sequences in three-dimensional space to reflect their relatedness. The cluster map generated for the MID-domain sequences of the Argonaute/PIWI protein family members (with a 10^{-10} P-value cutoff) (Fig. 1d) showed a pattern that is strikingly similar to that previously observed for analysis of the full-length protein[20,21]. Close examination of the MID-derived clades reveals that their sequence relatedness reflects the known divergence in functionality of these proteins, rather than simply grouping them by organism. In a rather tight and separate cluster are found all Argonaute proteins proposed to be involved in translational repression (DmAgo1, HsAgo1-4 and CeAlg1/2), while DmAgo2 and CeRde1, as well as many others, clearly are not included in this group. Using the same stringency cut-off (10^{-10}), neither full-length Argonaute sequences nor the isolated PAZ and PIWI domains separate into more than two very broad clusters (Supplementary Fig. 3a-c).

These computational results are striking and suggest that the MID domain is central to the functional distinctions that define the various Argonaute protein family members. We suggest that these groupings (shown more clearly in Supplementary Fig. 3d where stringency was increased to 10^{-20}) have considerable predictive power for the assignment of function to other

Argonautes. Apart from the clear distinction between Argonaute MID domains that are involved in miRNA-mediated translational repression and all other Argonautes, we also note, for example, that plant Argonautes are grouped based on their preference for the 5' miRNA nucleotide[22]. Interestingly, the clustering results do not group together all Argonaute proteins that can interact with the GW repeat proteins (GW182, TNRC6B, AIN-1 and Tas3), some of which are involved in translational repression (DmAgo1, HsAgo1-4, CeAlg1,2) while others are not (S. pombe or A. fulgidus Argonautes)[11,23-26] (Supplementary Fig. 3d). Based on these bioinformatic results, we predicted that there might be distinctive biochemical signatures associated with these species that could be probed through *in vitro* and *in vivo* analysis.

MID domains display distinct binding competition profiles

As a starting point, we expressed and purified MID domains from several species (*D. melanogaste*r (Dm), *C. elegans* (Ce) and *H. sapiens* (Hs)) as MBP-fusions in *E. coli*. The choices were guided by an interest in parsing differences between the two small RNA pathways: the miRNA mediators (*e.g.* DmAgo1, CeAlg1/2 and HsAgo1-4) and siRNA mediators (*e.g.* DmAgo2 and CeRde1). As controls, we used DmeIF4E and the C-terminal part of the *E. coli PurR* transcription regulator which contains two copies of a MID-like structural domain that binds diverse purine substrates[27]. We examined the ability of the various "MID" domains to bind "cap" by incubating cell lysates or purified proteins with m^7GTP-Sepharose (a partial mimic of authentic m^7GpppG cap structure) or GTP-Sepharose. All of the MID domains, as well as the ligand-binding domain of *PurR*, were able to bind to both resins (m^7GTP- and GTP-Sepharose), though with differing affinities (Fig. 2a and Supplementary Fig. 4a). We note that the miRNA-related Argonautes (DmAgo1, CeAlg1) consistently bound more effectively to m^7GTP-Sepharose than the siRNA-related Argonautes (DmAgo2, CeRde1) or the *PurR* domain (Fig. 2a). These observations are consistent with the expectation that each of these proteins would generally bind nucleotides, albeit with different relative affinities (*i.e.* PurR would be expected to prefer purine bases relative to pyrimidines, but might not discriminate against a methyl group at position 7, as previously reported27). As anticipated, the binding of DmeIF4E to m^7GTP-Sepharose was highly efficient (Supplementary Fig. 4b), and was specifically competed by cap related nucleotide analogs (data not shown).

We next asked whether binding to the various resins (m^7GTP and GTP-Sepharose) could be competed by free nucleotide analogs. As anticipated, PurR binding to each resin was easily competed by both GTP and m^7GpppG (data not shown); in addition, DmAgo2-MID binding was also readily competed by GTP (Fig. 2b). These observations are consistent with the idea that for DmAgo2, m^7GTP-Sepharose (or GTP-Sepharose) binding is mediated through the known 5'-end miRNA binding site located within the MID domain[28,29].

Interestingly, DmAgo1-MID binding was not easily competed with any single nucleotide tested (including GTP, GMP, GpppG and m^7GpppG), and moreover, binding was often stimulated by the addition of these nucleotides (Fig. 2c and Supplementary Fig. 4c,d). CeAlg1-MID behaved similarly (Figure 2c and Supplementary Fig. 4d). These data were puzzling, and, we realized, might be rationalized by the existence of two allosterically regulated nucleotide binding sites for these particular MID domains (DmAgo1 and CeAlg1). Consistent with this idea, we found in a more complete competition analysis that binding of DmAgo1 and CeAlg1 to m^7GTP-Sepharose was only effectively blocked by simultaneous pre-incubation with two different nucleotides, one cap like and the other not (Supplementary Fig. 4c,d). While it seemed obvious that one of these proposed nucleotide binding sites must correspond to the previously defined 5' miRNA binding site[28,29], it was less clear what the purpose or identity of the second site might be, though earlier studies on a potential cap binding activity of the Argonaute proteins were intriguing in this regard[4,30].

DmAgo1 cap resin binding is stimulated by miRNAs

The potential allostery and binding models were further explored in the context of full-length Argonaute proteins, DmAgo1, and an N-terminally truncated version of DmAgo2 (DmAgo2ΔQ, missing the N-terminal Q rich region), again expressed as MBP-fusions in *E. coli*. Both proteins were functional in standard RNA cleavage assays, indicating proper folding (Supplementary Fig. 5a). We next performed binding experiments with the same solid phase resins (GTP-, GMP- and m^7GTP-Sepharose) anticipating that increased specificity might now be observed in the context of the full-length proteins: we predicted that the 5' miRNA binding site would preferentially bind the GTP- and GMP-Sepharose resins, while the other site might preferentially bind the m^7GTP-Sepharose. Moreover, it seemed possible that miRNAs would be particularly effective at triggering the binding events if allostery existed.

These general trends were clearly seen when binding to these matrices was directly compared in the presence and absence of an authentic miRNA substrate (23 nts in length) and cap analog (m^7GpppG) (Fig. 2d). DmAgo2ΔQ binds poorly to m^7GTP, and better to GTP- and GMP-Sepharose (Fig. 2d); we argue that this binding is through the 5' miRNA binding site since it is effectively competed by miRNA. By contrast, DmAgo1 binds effectively to all three resins (in the case of m^7GTP, only when a miRNA is simultaneously bound). Most significantly, the competition profiles of DmAgo1 and DmAgo2 on m^7GTP-Sepharose are strikingly distinct from one another (Fig. 2d). Cap analogs have no effect on DmAgo1 GTP- or GMP-Sepharose binding while they readily compete with miRNA-stimulated m^7GTP-Sepharose binding. Together these data provide strong support for the idea that the miRNA-related Argonaute proteins (*e.g.* DmAgo1) have two distinct, allosterically regulated binding sites for nucleic acid, one for small RNAs and their mimics (here, GTP and GMP) and the other for cap like species (*e.g.* m^7GpppG and m^7GMP; see Supplementary Fig. 5b). As anticipated, we see dose dependent stimulation of m^7GTP-Sepharose binding by miRNAs (Fig. 2e).

Solution studies confirm allostery seen for DmAgo1

While the previous approaches provided us with a qualitative sense of allostery in DmAgo1, we were eager to test our models in more quantitative solution based binding experiments. Any allosteric model predicts that binding in either proposed site will stimulate binding in the other. To examine this, we developed filter-binding assays that monitored the binding of different radiolabeled RNA substrates. First, a short miRNA substrate was labeled at its 5' end and binding to DmAgo1 and DmAgo2ΔQ was evaluated (we used *bantam* as a model miRNA). Binding of the miRNA to both DmAgo1 and DmAgo2ΔQ was robust and direct competition experiments with unlabeled RNAs of varying lengths revealed their preference for miRNA-length substrates (~23 nts) (Fig. 3a,b). These data confirm that the purified Argonaute proteins have a small RNA binding site with properties that match known substrates (*e.g.* ref. 31). These experiments were also performed using a labeled duplex RNA (with *bantam* hybridized to its 2'-O-methylated complement). Overall binding of the duplex is higher affinity, but the same general pattern of length dependence is observed (Supplementary Fig. 6a,b). The higher affinity of the duplex could have important implications for the role of allostery in triggering downstream events in the pathway.

We next asked whether the binding of miRNAs to DmAgo1 and DmAgo2ΔQ was stimulated (or inhibited) by free nucleotide substrates. We began with DmAgo1 and performed the binding experiment under conditions where miRNA binding is initially inefficient, and observed approximately 3 fold stimulation of binding by numerous triphosphate-containing nucleotides (m^7GpppG, GpppG, GTP), but not by the monophosphate derivative GMP or the dinucleotide derivative NAD (Fig. 3c). At high levels of all nucleotides, including the triphosphates that stimulate binding in the putative cap site, competition with the labeled miRNA was eventually observed. Our data in this solution based assay argue that the 5' binding site has the following

specificity, miRNA>GMP>GTP>m^7GpppG, while the putative cap site has distinct specificity, m^7GpppG>GpppG>GTP>GMP. From a biochemical perspective, the observation that a given nucleotide can bind both sites with some affinity is not surprising. As seen for the purified MID domain, allosteric behavior was not observed for DmAgo2ΔQ, though GMP could compete at high concentrations (Fig. 3d). Similar results for DmAgo1 and DmAgo2ΔQ were seen when these same experiments were performed with the more tightly binding duplex (Supplementary Fig. 6c, d).

In a complementary set of experiments, we evaluated the binding of radiolabeled capped and uncapped mRNA species as a function of miRNA duplex concentration. Again consistent with an allosteric model, miRNA duplex (miRNA*) stimulated DmAgo1 binding to capped mRNAs by 10 fold whereas the same RNA species had no effect on DmAgo2ΔQ binding (Fig. 3e). Moreover, the observed miRNA duplex-triggered stimulation of DmAgo1 binding to labeled mRNAs was more effective for capped (m^7GpppG) mRNA species than for those initiated with either pppG or pG (Supplementary Fig. 6e), a trend consistent with the rankings described above. Competition experiments were next performed in order to evaluate the relative affinities of a series of cap like compounds. Various nucleotide analogs were added to the DmAgo1 binding mixture (with saturating miRNA duplex and ^{32}P-labeled capped mRNA) (Fig. 3f). Authentic cap (m^7GpppG) was the most effective competitor of mRNA binding, followed by GpppG, GTP and GMP.

In vivo analysis identifies potential cap site on DmAgo1

To assess the *in vivo* functional relevance of our *in vitro* observations, we employed a previously developed luciferase-based reporter system, here in *Drosophila* S2 cells, to probe the known function of DmAgo1 in translational repression[30,32]. In these experiments the Argonaute is targeted directly to the mRNA of interest through a fused binding domain (the *lambda* N protein), allowing mutations in the Argonaute protein to be directly evaluated in the presence of endogenous Argonaute protein. As anticipated from their distinct roles in miRNA-mediated and siRNA-mediated gene regulation[33], DmAgo1 effectively repressed firefly luciferase expression in the tethered system whereas DmAgo2ΔQ did not (Fig. 4a). In an initial characterization, we found that neither increasing effector amount (the Argonaute fusion protein) nor decreasing reporter amount (F-Luc-5boxB) had any impact on the observed extent of repression (data not shown); these data suggest that all sites on the mRNA reporter are occupied by the Argonaute fusion protein, and that the results shed light on core functional properties of the protein.

This assay was then used to identify mutations in the MID domain that might report on the two distinct binding sites identified through *in vitro* biochemistry. We looked to the structurally related proteins with Rossmann-like folds for clues, as many of these proteins have two distinct allosterically regulated ligand-binding sites[18] (Supplementary Fig. 7). The first of the conserved binding sites is the known 5'-endmiRNA binding site of the Argonautes, located within the last αβα-element of the domain (Fig. 4b). Two conserved amino acids, Y619 and K623 (shown in green), that stack with the first nucleotide of the guide RNA and interact with its 5' phosphate, respectively[29], were mutated and their effects on repression evaluated. Amino acid substitutions at either position (Y619L or K623E) substantially derepressed the reporter, while a change in both positions (YK) yielded full derepression (Fig. 4c). These results were initially surprising given that direct tethering of DmAgo1 to the reporter might be expected to obviate the need for miRNA binding. We propose that these results are fully consistent with the allosteric mechanism for DmAgo1 function proposed above: miRNA binding is essential for promoting interactions in a second binding site (and/or for recruiting additional proteins such as GW182) that are somehow important in specifying translational repression.

These mutants have previously been characterized *in vitro* where they showed compromised binding to miRNAs and modestly reduced cleavage of mRNAs (ref. 28); here, when miRNAs are supplied in saturating concentrations, the YK mutant protein efficiently cleaves mRNA targets (Supplementary Fig. 8). These data argue that the proteins are folded and functional, consistent with the stable protein that we see expressed in our S2 cells (Fig. 4c).

Further examination of potential ligand-binding sites pointed to the loop regions found at either end of the MID domain (*e.g.* see ligands in Supplementary Fig. 7). We took an unbiased approach and mutated strings of amino acids in these loops (see Supplementary Fig. 9a). When we evaluated these mutants in the reporter assay (Supplementary Fig. 9b), we found that only mutation of a single loop connecting the third helix and fourth beta strand (residues 627-630) resulted in substantial derepression of the reporter construct. More refined mutational analysis identified a single conserved residue, D627 (Fig. 4b, orange), mutation of which to a lysine fully abolished repression, while mutation to a like-charged glutamate mostly maintained function (Fig. 4d). As above, *in vitro* cleavage assays confirmed that this variant protein (D627K) is folded and functional, though with anticipated defects in m^7GTP-Sepharose binding (Supplementary Fig. 8 and 9c); this mutationally sensitive position represents a single mutation in a surface-located residue of a large protein. Since the distance between D627 and the 5'-end-miRNA site is about 15 Å, it seems unlikely that position D627 plays a direct role in binding of the 5' end of the miRNA. We propose that D627 is found in a second site important for allostery, and potentially one that binds to mRNA caps to participate in translational repression.

Coupled interactions of DmAgo1 with cap, miRNA and GW182

To more fully define the molecular defects of the Argonaute variants, we evaluated their ability to bind miRNAs and cap in cellular S2 lysates. To evaluate miRNA binding, HA-tagged wild type DmAgo1 (WT) and several variants were transfected and immunoprecipitated from cells and the amount of *bantam* miRNA bound was assessed by northern blot[30,34]. While all DmAgo1 variants were expressed, the two non-repressing DmAgo1 variants (the YK double mutant in the 5'-end-miRNA site and D627K in the putative cap site) showed no detectable binding to the *bantam* miRNA, whereas all functional, repressing variants exhibited potent miRNA binding (*e.g.* WT, K615E, D627E and K640A) (Fig. 4e). We also included in this analysis several controls: DmAgo2ΔQ (ΔQ), mutations in the putative "4E" homologous phenylalanines[4] (dblA) of DmAgo1, and DmeIF4E (4E), none of which bound miRNA effectively. These data, combined with other functional studies (our own in Supplementary Fig. 10a and ref. 30) and the bioinformatics presented here (and in ref. 35), make clear that the Argonaute proteins and eIF4E are not directly related.

The same set of S2 cell expressed Argonaute protein variants revealed similar trends in an m^7GTP-Sepharose pull-down assay. Variants that are active in the tethering assay bind the m^7GTP resin effectively (*e.g.* WT, K615E, D627E and K640A), whereas those variants that are inactive do not (Fig. 4f). The non-repressing DmAgo2ΔQ, the double phenylalanine DmAgo1 (dblA), and DmeIF4E (4E) serve as controls for this experiment.

In an attempt to reconcile our results with much literature surrounding the role of GW182 in repression, we examined the effects of these same mutations on binding to this protein using a co-immunoprecipitation assay in S2 cells (Supplementary Fig. 10b); these data indicate that GW182 binding directly correlates with both cap and miRNA binding. The correlation that we observe in the three different *in vivo*-based assays is striking: variants that repress the tethered reporter bind miRNA, cap resin and GW182; conversely, variants that fail to repress translation fail to bind all three substrates. The *in vitro* functionality of these variant proteins (Supplementary Fig. 8 and 9c) and the conservative nature of the amino acid substitutions lend weight to the importance of these results.

DISCUSSION

The computational and biochemical results presented here provide new insights into Argonaute function. The MID domain stands out computationally in identifying functionally relevant groupings of Argonaute proteins (across organismal boundaries), while our biochemistry argues for functionally distinctive behavior of the Argonaute proteins that reports on MID domain's mechanistic features. We propose that the subclass of the Argonaute protein family involved in miRNA-mediated gene regulation (DmAgo1, CeAlg1/2, HsAgo1-4) depends on allostery to modulate binding to at least two distinct ligands, a miRNA and an mRNA cap (Figure 5). Such allostery could allow this family of proteins to trigger translational repression through cap binding when loaded with a miRNA engaged on an authentic target[4,36]. Alternatively, the allostery could be used during the miRNP loading phase where the Argonaute is deciphering the miRNA:mRNA duplex in the process of target identification[37-39].

We cannot exclude the possibility that the potential cap-binding site is normally occupied by free nucleotides or other RNA species in the cell. For example, such an allosteric site might provide a route for the regulation of miRNA-mediated events during certain stages in the cell cycle40 (correlated with cellular nucleotide levels, for example, ref. 41) or in certain cellular environments. We note that the binding affinities of DmAgo1 for free nucleotides are substantially lower than for intact mRNA-like species, arguing against such more speculative models.

In either of the above models, effects on repression could be manifested through interactions with GW182 or other factors (Figure 5). Indeed, there is considerable evidence supporting an essential role for GW182 (and its homologs, *H. sapiens* TNRC6B and *C. elegans* AIN-1) in mediating translational repression[11-13,21,42]. Moreover, a number of studies argue for a direct connection between miRNA loading and downstream functional consequences42-44, while some others suggest that such coupling is not essential12,25. Here, mutations in the 5'-miRNA binding site simultaneously abrogate GW182 and miRNA binding (and also cap binding), and in turn fail to repress target mRNA translation. From these data alone, we are unable to determine the root cause for the loss of translational repression. One recent study described DmAgo1 mutants with impaired GW182 binding and unaffected miRNA binding that retain the ability to partially repress multiple mRNA targets[12]; these studies leave open the possibility that both GW182 and cap binding can contribute to translational repression6,7. These ideas are also consistent with recent reports from the Hentze group8. A parsimonious model for these diverse results would invoke the coupling of all three elements through the Argonaute protein, miRNA, cap and GW182, all present in the cell at somewhat limiting concentrations, and where binding of any induces the cooperative assembly of the repressive complex (outlined hypothetically in Figure 5). These ideas make a number of specific predictions that can be tested.

The allostery that we document is appealing for a number of reasons. First, the Argonaute proteins are distantly related to a large group of proteins having a Rossmann-like fold, a number of which have two distinct ligand binding domains that are allosterically regulated[18]. A particularly interesting example is the protein *PyrR* that binds pyrimidine nucleotides in one site and regulates downstream transcription through interactions with an RNA structure that is eerily similar to that of a miRNA bound to its target[45]. Recent structures of *T. thermophilus* Argonaute show conformational changes in the MID/PIWI domains upon binding of various miRNA species[46-48]. The authors argue that rotation allows better accommodation of the guide strand between the 5' miRNA binding site and the PIWI domain, but could also affect elements in the MID and PIWI domain important for binding cap and/or GW182, or other molecular players. For example, it seems plausible that a similar mechanism is in play in *C. elegans* where nRDE-3 Argonaute redistributes from the cytoplasm to the nucleus only upon binding to

siRNAs[49]. Our observations provide a biochemical read-out for these structural changes – allostery – and argue for the relevance of this mechanistic feature for *in vivo* function.

Methods

Bioinformatic analysis

We collected sequences of the Argonaute/PIWI-MID domains using PSI-BLAST searches of the NCBI NR database. We used different MID-domains from eukaryotic Argonautes as PSI-BLAST queries (E-value cutoff 0.001, maximum 11 rounds, NR database). We performed additional sequence-structure analysis using HHpred[14] and BioInfoBank Meta-Server50. We aligned sequences of different MID-domains using ClustalW51, HHpred, 3D-Jury50 and adjusted them by hand using secondary structure predictions (Supplementary Fig. 1).

We built structure models for the DmAgo1-MID domain (gi: 17647145, residues 538-665) using the alignment interface of SWISS-MODEL workspace[52] and structures of *A. fulgidus* PIWI-domains (PDB: 1w9h and PDB: 2bgg) as templates. We used DALI server[17] to perform a structure-based search on the MID domain from *A. fulgidus* (PDB:1w9h) (Supplementary Fig. 2a).

We performed clustering of sequences using the CLANS application[19] on the sample of sequences we collected from the PSI-BLAST searches using DmAgo1-MID, PAZ and PIWI domains. We chose a set of 834 sequences that contained all three conserved PAZ, MID and PIWI domains. These sequences were clustered in 3D space for approximately 5000 rounds using the same P-value cutoff (10^{-10}) for either full length protein or individual domain sequences. Argonaute MID domains were also clustered using a P-value cutoff of 10^{-20}.

Binding to m^{7}GTP-, GTP- and GMP-Sepharose beads

We diluted purified MBP-MID proteins, DmeIF4E and PurR-C into 200 μl of PBS with 5 mM $MgCl_2$. When indicated, we added m^{7}GpppG (NEB), m^{7}GMP (Jena Bioscience), GpppG (NEB), GTP and GMP (Amersham), or a combination thereof, to a final concentration of 500 μM. We incubated the samples for 15 minutes at 4° C prior to addition of 30 μl of m^{7}GTP- (GE-Healthcare), GTP-, or GMP-Sepharose beads (Sigma), followed by rotation for 2 hours at 4° C. We washed the beads four times with 600 μl of PBS, 2 mM $MgCl_2$, and heparin (0.5 mg/ml) and eluted bound proteins with sample buffer. We analyzed the elutions either by colloidal Coomassie Blue staining or western blotting. For the miRNA stimulation/competition experiments, we incubated DmAgo1 and DmAgo2ΔQ with saturating amounts of *bantam* miRNA prior to the binding experiment.

Labeling of RNAs

We prepared radiolabeled *bantam* using T4 polynucleotide kinase (PNK) (NEB) and [γ-^{32}P]-ATP (PerkinElmer)[53], and then purified it by denaturing PAGE. We prepared radiolabeled duplex by mixing radiolabeled *bantam* with antisense oligonucleotide (antagomir in ref. 54). We annealed the mixture and treated with S1 nuclease (Invitrogen) to remove remaining single stranded oligonucleotide and purified labeled duplex by native PAGE.

We prepared radiolabeled capped mRNA species according to a modified protocol from ref. [55]. We made [^{32}P]-GpppG, [^{32}P]-m^{7}GpppG and [^{3}H]-m^{7}GpppG species using [α-^{32}P]-GTP or [methyl-^{3}H]-Adenosyl-L-methionine (PerkinElmer), respectively, in the capping mixture. We purified [^{32}P]-GpppG and [^{32}P]-m^{7}GpppG mRNAs by denaturing PAGE and purified [^{3}H]-m^{7}GpppG mRNA using Illustra™ MicroSpin G-25 Columns (GE Healthcare), since we noticed cap instability in [^{32}P]-m^{7}GpppG mRNA during gel purification.

We radiolabled “uncapped” mRNA species (pG and pppG) at 3’ ends using [^{32}P]-pCp and T4 RNA ligase (Promega) according to the manufacturer's instructions, then purified the labeled RNA transcripts by denaturing PAGE.

Filter binding assays

We performed competition experiments with RNAs of several different lengths using a constant amount of the assayed protein and labeled *bantam* or duplex miRNA. We premixed varying amounts of non-labeled RNA and a constant amount of labeled *bantam* or duplex in PBS with 5 mM $MgCl_2$, then added protein and incubated the mixture at room temperature for 30 minutes. We performed stimulation experiments with nucleotide substrates by premixing a constant amount of assayed protein with varying amounts of nucleotide substrates, and then incubating at room temperature for 10 minutes. We then added labeled *bantam* or duplex and incubated the mixtures for an additional 30 minutes. We performed experiments with “capped” and “uncapped” mRNA species by premixing assayed protein with *bantam* or duplex and incubating the mixture at room temperature for 30 minutes. We then added labeled mRNA species and incubated the mixtures for an additional 10 minutes. Where indicated, we premixed nucleotide substrates with mRNA species. We performed filter binding assays by[56], using 400 μl of assay buffer for washing steps.

Cell Culture and Transfections

We cultured *Drosophila* S2 cells in Express Five SFM Medium (Invitrogen) supplemented with 100 units/ml penicillin, 100 units/ml streptomycin (Cambrex BioScience) and 45 ml of 200 mM L-glutamine (Invitrogen) per 500 ml medium. We performed all transfections using Effectene (Qiagen). For luminometer assays, we seeded cells in 24-well plates and transfected in triplicate. Each well contained 5 ng F-Luc reporter plasmid, 5 ng R-Luc control plasmid, and 200 ng effector plasmid. We processed samples 3 days post-transfection with the Dual Luciferase Reporter Assay System (Promega).

For HA immunoprecipitation/miRNA northerns, we seeded cells in 15 cm dishes and transfected using 15 μg HA-tagged construct and 15 μg *bantam* construct. For the GW182 co-immunoprecipitation experiment, we transfected using 2 μg of the chosen construct(s). For m^{7}GTP-Sepharose pull-downs, we seeded cells in 10 cm dishes and transfected using 10 μg HA-tagged construct. We harvested cells 3 days post-transfection.

S2 cell immunoprecipitations and m^{7}GTP-Sepharose pull-downs

For HA-immunoprecipitation (IP), we lysed cells with Buffer A (20 mM Tris-HCl (pH 7.4), 200 mM NaCl, 2.5 mM $MgCl_2$, 0.1% NP-40, Complete Protease Inhibitor (Roche), RNasin (Promega)), sonicated, and clarified. Of the cleared lysate, we reserved two aliquots for western analysis and RNA extraction. We used the rest for immunoprecipitation with Protein G-Agarose (Roche) and a monoclonal anti-HA-HRP antibody (Santa Cruz Biotechnology). We washed the resin with Wash Buffer (Buffer A with 100 mM NaCl and 0.05% NP-40), reserved a final aliquot for western analysis, and used the rest for RNA extraction. For m^{7}GTP-Sepharose pull-downs, we lysed cells with Buffer B (50 mM Tris-HCl (pH7.4), 150 mM NaCl, 1 mM EDTA, 0.1% Triton X-100, Complete Protease Inhibitor), sonicated, and clarified. Of the cleared lysate, we reserved two aliquots as input and for HA IP as described above. We used the rest for pull-downs with m^{7}GTP-Sepharose (GE Healthcare). We washed the resin with Buffer B and resuspended the pellets in sample buffer. For GW182 co-IPs, we used either the anti-HA-HRP or a monoclonal anti-FLAG antibody (Sigma) as indicated.

Supplementary Material

Refer to Web version on PubMed Central for supplementary material.

Acknowledgments

We thank S. Dorner for early contributions to the project, E. Izaurralde (Max Planck Institute, Tübingen, Germany) for providing the luciferase reporter constructs, H. Zaher for mRNA constructs used in filter binding assays, and J. Mendell, G. Seydoux, J. Lorsch, L. Cochella and H. Zaher for helpful comments on the manuscript. J.K.H. was supported by The Samsung Foundation of Culture. The project was supported by funding from HHMI.

References

1. Ghildiyal M, Zamore PD. Small silencing RNAs: an expanding universe. Nature Reviews Genetics 2009;10:94–108.
2. Carthew RW, Sontheimer EJ. Origins and Mechanisms of miRNAs and siRNAs. Cell 2009;136:642–55. [PubMed: 19239886]
3. Wu L, Belasco JG. Let me count the ways: mechanisms of gene regulation by miRNAs and siRNAs. Mol Cell 2008;29:1–7. [PubMed: 18206964]
4. Kiriakidou M, et al. An mRNA m(7)G cap binding-like motif within human Ago2 represses translation. Cell 2007;129:1141–1151. [PubMed: 17524464]
5. Pillai RS, et al. Inhibition of translational initiation by Let-7 MicroRNA in human cells. Science 2005;309:1573–6. [PubMed: 16081698]
6. Humphreys DT, Westman BJ, Martin DI, Preiss T. MicroRNAs control translation initiation by inhibiting eukaryotic initiation factor 4E/cap and poly(A) tail function. Proc Natl Acad Sci U S A 2005;102:16961–6. [PubMed: 16287976]
7. Wakiyama M, Takimoto K, Ohara O, Yokoyama S. Let-7 microRNA-mediated mRNA deadenylation and translational repression in a mammalian cell-free system. Genes Dev 2007;21:1857–62. [PubMed: 17671087]
8. Zdanowicz A, et al. Drosophila miR2 primarily targets the m7GpppN cap structure for translational repression. Mol Cell 2009;35:881–8. [PubMed: 19782035]
9. Wang B, Love TM, Call ME, Doench JG, Novina CD. Recapitulation of short RNA-directed translational gene silencing in vitro. Mol Cell 2006;22:553–60. [PubMed: 16713585]
10. Wang B, Yanez A, Novina CD. MicroRNA-repressed mRNAs contain 40S but not 60S components. Proc Natl Acad Sci U S A 2008;105:5343–8. [PubMed: 18390669]
11. Rehwinkel J, Behm-Ansmant I, Gatfield D, Izaurralde E. A crucial role for GW182 and the DCP1:DCP2 decapping complex in miRNA-mediated gene silencing. RNA 2005;11:1640–7. [PubMed: 16177138]
12. Eulalio A, Helms S, Fritzsch C, Fauser M, Izaurralde E. A C-terminal silencing domain in GW182 is essential for miRNA function. RNA 2009;15:1067–77. [PubMed: 19383769]
13. Chekulaeva M, Filipowicz W, Parker R. Multiple independent domains of dGW182 function in miRNA-mediated repression in Drosophila. RNA 2009;15:794–803. [PubMed: 19304924]
14. Soding J, Biegert A, Lupas AN. The HHpred interactive server for protein homology detection and structure prediction. Nucleic Acids Res 2005;33:W244–8. [PubMed: 15980461]
15. Song JJ, Smith SK, Hannon GJ, Joshua-Tor L. Crystal structure of argonaute and its implications for RISC slicer activity. Science 2004;305:1434–1437. [PubMed: 15284453]
16. Marcotrigiano J, Gingras AC, Sonenberg N, Burley SK. Cocrystal structure of the messenger RNA 5' cap-binding protein (eIF4E) bound to 7-methyl-GDP. Cell 1997;89:951–961. [PubMed: 9200613]
17. Holm L, Sander C. Protein-Structure Comparison by Alignment of Distance Matrices. Journal of Molecular Biology 1993;233:123–138. [PubMed: 8377180]
18. Anantharaman V, Aravind L. Diversification of catalytic activities and ligand interactions in the protein fold shared by the sugar isomerases, eIF2B, DeoR transcription factors Acyl-CoA transferases and methenyltetrahydrofolate synthetase. Journal of Molecular Biology 2006;356:823–842. [PubMed: 16376935]
19. Frickey T, Lupas A. CLANS: a Java application for visualizing protein families based on pairwise similarity. Bioinformatics 2004;20:3702–3704. [PubMed: 15284097]

20. Carmell MA, Xuan Z, Zhang MQ, Hannon GJ. The Argonaute family: tentacles that reach into RNAi, developmental control, stem cell maintenance, and tumorigenesis. Genes Dev 2002;16:2733–42. [PubMed: 12414724]
21. Parker JS, Barford D. Argonaute: a scaffold for the function of short regulatory RNAs. Trends in Biochemical Sciences 2006;31:622–630. [PubMed: 17029813]
22. Mi S, et al. Sorting of small RNAs into Arabidopsis argonaute complexes is directed by the 5' terminal nucleotide. Cell 2008;133:116–27. [PubMed: 18342361]
23. Verdel A, et al. RNAi-mediated targeting of heterochromatin by the RITS complex. Science 2004;303:672–6. [PubMed: 14704433]
24. Meister G, et al. Identification of novel argonaute-associated proteins. Curr Biol 2005;15:2149–55. [PubMed: 16289642]
25. Till S, et al. A conserved motif in Argonaute-interacting proteins mediates functional interactions through the Argonaute PIWI domain. Nat Struct Mol Biol 2007;14:897–903. [PubMed: 17891150]
26. Ding L, Spencer A, Morita K, Han M. The developmental timing regulator AIN-1 interacts with miRISCs and may target the argonaute protein ALG-1 to cytoplasmic P bodies in C. elegans. Mol Cell 2005;19:437–47. [PubMed: 16109369]
27. Schumacher MA, Choi KY, Zalkin H, Brennan RG. Crystal structure of LacI member, PurR, bound to DNA: minor groove binding by alpha helices. Science 1994;266:763–70. [PubMed: 7973627]
28. Ma JB, et al. Structural basis for 5 '-end-specific recognition of guide RNA by the A-fulgidus Piwi protein. Nature 2005;434:666–670. [PubMed: 15800629]
29. Parker JS, Roe SM, Barford D. Structural insights into mRNA recognition from a PIWI domain-siRNA guide complex. Nature 2005;434:663–666. [PubMed: 15800628]
30. Eulalio A, Huntzinger E, Izaurralde E. GW182 interaction with Argonaute is essential for miRNA-mediated translational repression and mRNA decay. Nature Structural & Molecular Biology 2008;15:346–353.
31. Lagos-Quintana M, Rauhut R, Lendeckel W, Tuschl T. Identification of novel genes coding for small expressed RNAs. Science 2001;294:853–8. [PubMed: 11679670]
32. Pillai RS, Artus CG, Filipowicz W. Tethering of human Ago proteins to mRNA mimics the miRNA-mediated repression of protein synthesis. Rna-a Publication of the Rna Society 2004;10:1518–1525.
33. Rehwinkel J, et al. Genome-wide analysis of mRNAs regulated by Drosha and Argonaute proteins in Drosophila melanogaster. Mol Cell Biol 2006;26:2965–75. [PubMed: 16581772]
34. Okamura K, Ishizuka A, Siomi H, Siomi MC. Distinct roles for argonaute proteins in small RNA-directed RNA cleavage pathways. Genes & Development 2004;18:1655–1666. [PubMed: 15231716]
35. Kinch LN, Grishin NV. The human Ago2 MC region does not contain an eIF4E-like mRNA cap binding motif. Biology Direct 2009;4
36. Mathonnet G, et al. MicroRNA inhibition of translation initiation in vitro by targeting the cap-binding complex eIF4F. Science 2007;317:1764–7. [PubMed: 17656684]
37. Miyoshi K, Okada TN, Siomi H, Siomi MC. Characterization of the miRNA-RISC loading complex and miRNA-RISC formed in the Drosophila miRNA pathway. Rna. 2009
38. Miyoshi K, Tsukumo H, Nagami T, Siomi H, Siomi MC. Slicer function of Drosophila Argonautes and its involvement in RISC formation. Genes Dev 2005;19:2837–48. [PubMed: 16287716]
39. Tomari Y, Du T, Zamore PD. Sorting of Drosophila small silencing RNAs. Cell 2007;130:299–308. [PubMed: 17662944]
40. Vasudevan S, Tong Y, Steitz JA. Cell-cycle control of microRNA-mediated translation regulation. Cell Cycle 2008;7:1545–9. [PubMed: 18469529]
41. Tu BP, et al. Cyclic changes in metabolic state during the life of a yeast cell. Proc Natl Acad Sci U S A 2007;104:16886–91. [PubMed: 17940006]
42. Liu J, et al. A role for the P-body component GW182 in microRNA function. Nat Cell Biol 2005;7:1261–6. [PubMed: 16284623]
43. Liu J, Valencia-Sanchez MA, Hannon GJ, Parker R. MicroRNA-dependent localization of targeted mRNAs to mammalian P-bodies. Nat Cell Biol 2005;7:719–23. [PubMed: 15937477]
44. Pauley KM, et al. Formation of GW bodies is a consequence of microRNA genesis. EMBO Rep 2006;7:904–10. [PubMed: 16906129]

45. Turnbough CL Jr. Switzer RL. Regulation of pyrimidine biosynthetic gene expression in bacteria: repression without repressors. Microbiol Mol Biol Rev 2008;72:266–300. table of contents. [PubMed: 18535147]

46. Wang YL, et al. Structure of an argonaute silencing complex with a seed-containing guide DNA and target RNA duplex. Nature 2008;456:921–U72. [PubMed: 19092929]

47. Wang YL, Sheng G, Juranek S, Tuschl T, Patel DJ. Structure of the guide-strand-containing argonaute silencing complex. Nature 2008;456:209–U34. [PubMed: 18754009]

48. Wang Y, et al. Nucleation, propagation and cleavage of target RNAs in Ago silencing complexes. Nature 2009;461:754–61. [PubMed: 19812667]

49. Guang S, et al. An Argonaute transports siRNAs from the cytoplasm to the nucleus. Science 2008;321:537–41. [PubMed: 18653886]

50. Ginalski K, Elofsson A, Fischer D, Rychlewski L. 3D-Jury: a simple approach to improve protein structure predictions. Bioinformatics 2003;19:1015–8. [PubMed: 12761065]

51. Thompson JD, Higgins DG, Gibson TJ. CLUSTAL W: improving the sensitivity of progressive multiple sequence alignment through sequence weighting, position-specific gap penalties and weight matrix choice. Nucleic Acids Res 1994;22:4673–80. [PubMed: 7984417]

52. Arnold K, Bordoli L, Kopp J, Schwede T. The SWISS-MODEL workspace: a web-based environment for protein structure homology modelling. Bioinformatics 2006;22:195–201. [PubMed: 16301204]

53. Miyoshi K, Uejima H, Nagami-Okada T, Siomi H, Siomi MC. In vitro RNA cleavage assay for Argonaute-family proteins. Methods Mol Biol 2008;442:29–43. [PubMed: 18369776]

54. Nahvi A, Shoemaker CJ, Green R. An expanded seed sequence definition accounts for full regulation of the hid 3' UTR by bantam miRNA. RNA 2009;15:814–22. [PubMed: 19286629]

55. Cong PJ, Shuman S. Mutational Analysis of Messenger-Rna Capping Enzyme Identifies Amino-Acids Involved in Gtp-Binding, Enzyme-Guanylate Formation, and Gmp Transfer to Rna. Molecular and Cellular Biology 1995;15:6222–6231. [PubMed: 7565775]

56. Stockley PG. Filter-binding assays. Methods Mol Biol 2009;543:1–14. [PubMed: 19378155]

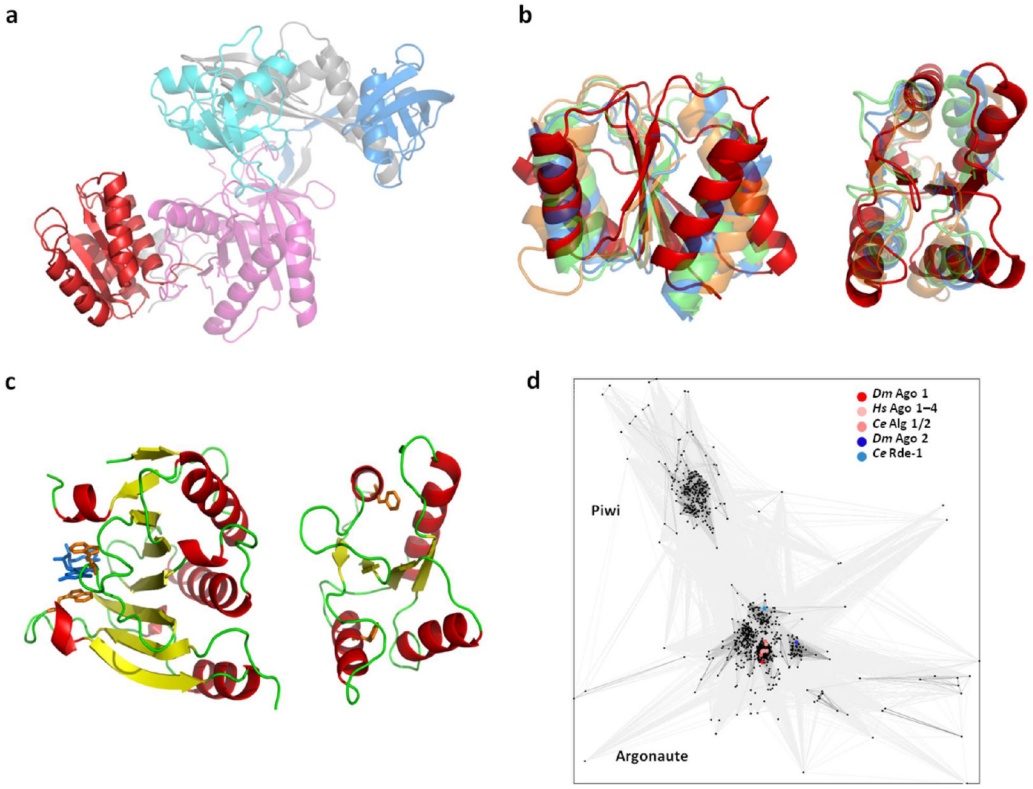

Figure 1.

Bioinformatic analysis of Argonaute proteins. **a,** Cartoon representation of the *T. Thermophilus* Argonaute (PDB: 3dlb) showing the N-terminal domain in cyan, PAZ domain in blue, MID domain in red and PIWI domain in magenta. **b,** Superimposition of the modeled DmAgo1 MID domain (red) with similar structures: N-domain of sugar transporter from *C. phytofermentans* (green, PDB: 3brs, residues 5-98 and 246-263), ligand binding domain of *E. coli PurR* purine repressor (blue, PDB: 2pua, residues 60-147 and 294-311) and ligand-sensitive negative regulator from *P. aeruginosa*, *AmiC* (orange, PDB: 1qo0, residues 127-232). **c,** Structure of the *M. musculus* eIF4E bound to m^7GDP (left, PDB: 1ej1, m^7GDP in blue) and modeled DmAgo1 MID domain (right). Tryptophan residues of eIF4E (W56 and W102), involved in binding of m^7GDP, and "equivalent" phenylalanine residues (F560 and F595) of modeled DmAgo1 MID domain are shown in orange. **d,** Cluster analysis of MID-domain sequences from Argonaute/PIWI protein family. Each sequence is represented by one dot. Darker lines represent pairwise connections with very low P-values and lighter ones those with higher values, closer to the cutoff (10^{-10}). Positions of protein sequences discussed in this study are labeled with colored dots.

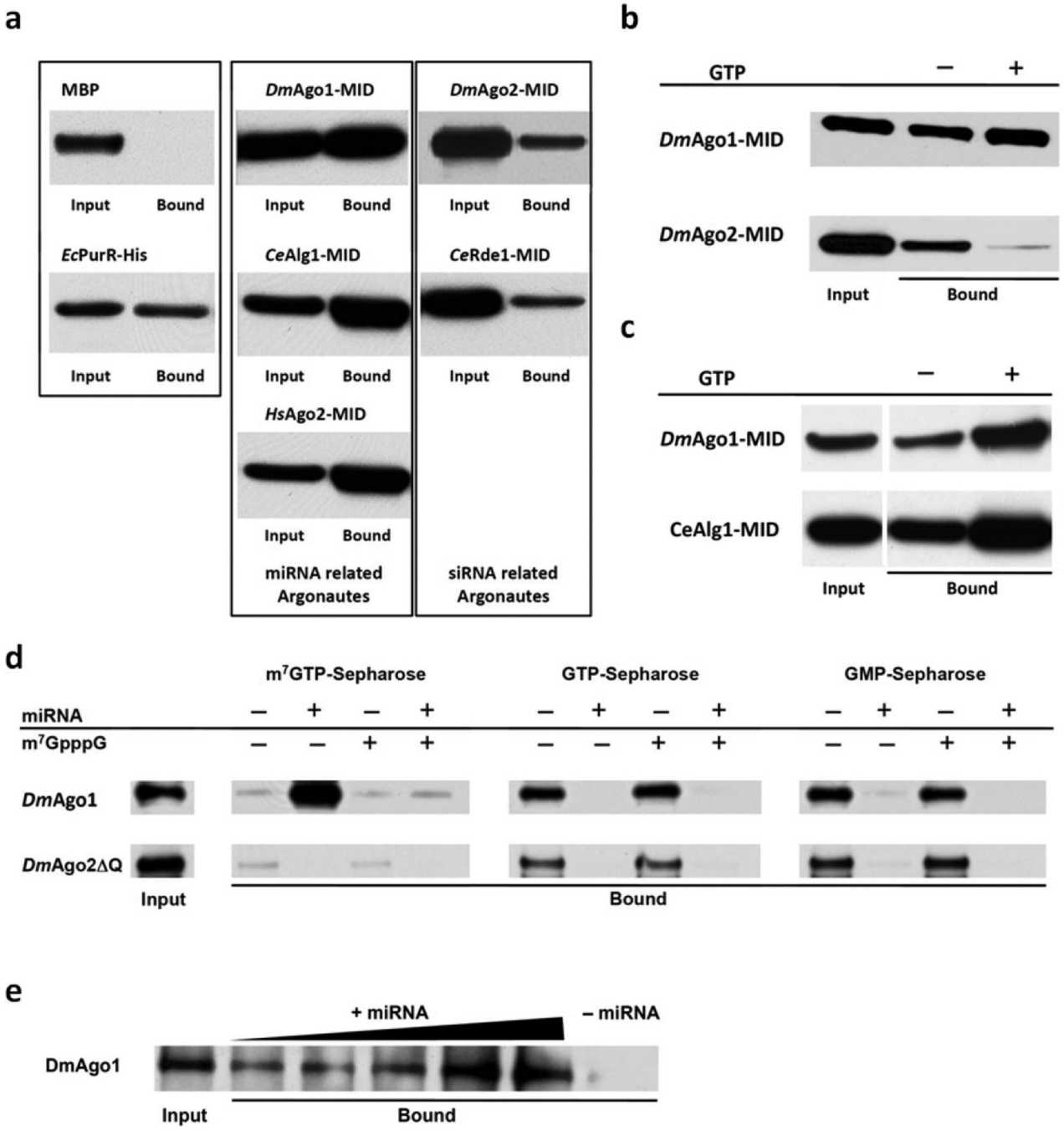

Figure 2.

Binding of Argonaute proteins to m^{7}GTP-Sepharose reveal allosteric behavior. **a,** Binding of purified Argonaute MID-domains and *PurR* protein to the m^{7}GTP-Sepharose (Dm, *D. melanogaster*; Ce, *C. elegans;* Hs, *H. sapiens*; Ec, *E. coli*). miRNA and siRNA related Argonautes are shown in separate boxes. MBP is used as a negative control. **b,** Binding of DmAgo1-MID and DmAgo2-MID domains to m^{7}GTP-Sepharose in the presence of GTP. The total amount of nucleotide is 500 μM, input (10%) and bound fraction (40%) were analyzed by western blotting. **c,** Binding of DmAgo1 and CeAlg1 MID domains to m^{7}GTP-Sepharose is stimulated by addition of 250 μM GTP. Input (10%) and bound fraction (50%) were analyzed by western blotting. **d,** Binding of full-length DmAgo1, and not of DmAgo2ΔQ, to m^{7}GTP-

Sepharose is specific and stimulated by addition of short RNA (23-mer). Binding to m^7GTP-resin is competed by addition of m^7GpppG. Binding of both, DmAgo1 and DmAgo2ΔQ, to GTP- and GMP-Sepharose is competed by addition of short RNA (23-mer). m^7GpppG shows no effect on binding to these resins. Input (20%) and bound fraction (25%) were analyzed by western blotting. **e,** Binding of full-length DmAgo1 to m7GTP-Sepharose in presence of increasing amounts of short RNA (23-mer). Input (20%) and bound fraction (20%) in assays were analyzed by western blotting using polyclonal anti-MBP (NEB) antibody.

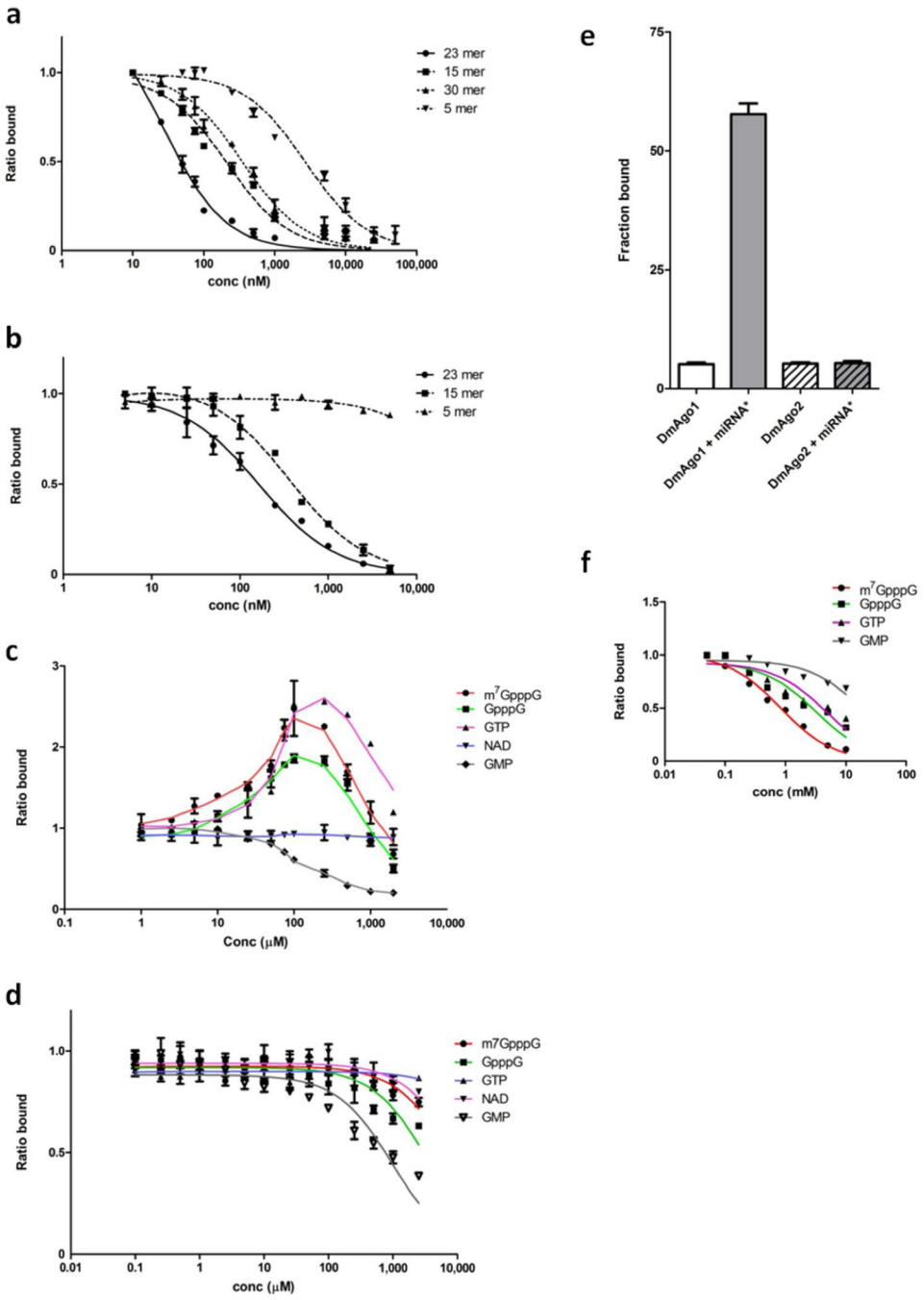

Figure 3.

Filter binding assays indicate two allosterically regulated nucleotide binding sites. Binding of ^{32}P-labeled *bantam* to DmAgo1 in **a** and DmAgo2ΔQ in **b** in the presence of non-labeled RNAs of varying lengths (5, 15, 23 and 30 nts). Competition between labeled and non-labeled RNAs was performed by titration of the non-labeled species and represented by the ratio of bound ^{32}P-*bantam* in the presence and absence of competing RNA species. Influence of different nucleotide substrates on the ^{32}P-*bantam* binding to DmAgo1 in **c** and DmAgo2ΔQ in **d**. Nucleotide substrates were titrated and the amount of the bound ^{32}P-*bantam* was followed. Values represent the ratio of bound ^{32}P-*bantam* in the presence and absence of indicated nucleotide substrate. **e,** Binding of *bantam* duplex (miRNA*) to DmAgo1 and DmAgo2ΔQ

stimulates only binding of DmAgo1 to ^{3}H-labeled m^{7}GpppG mRNA. **f,** Influence of different nucleotide substrates on binding of ^{3}H-m^{7}GpppG mRNA to DmAgo1. Error bars represent the standard error from at least three experiments.

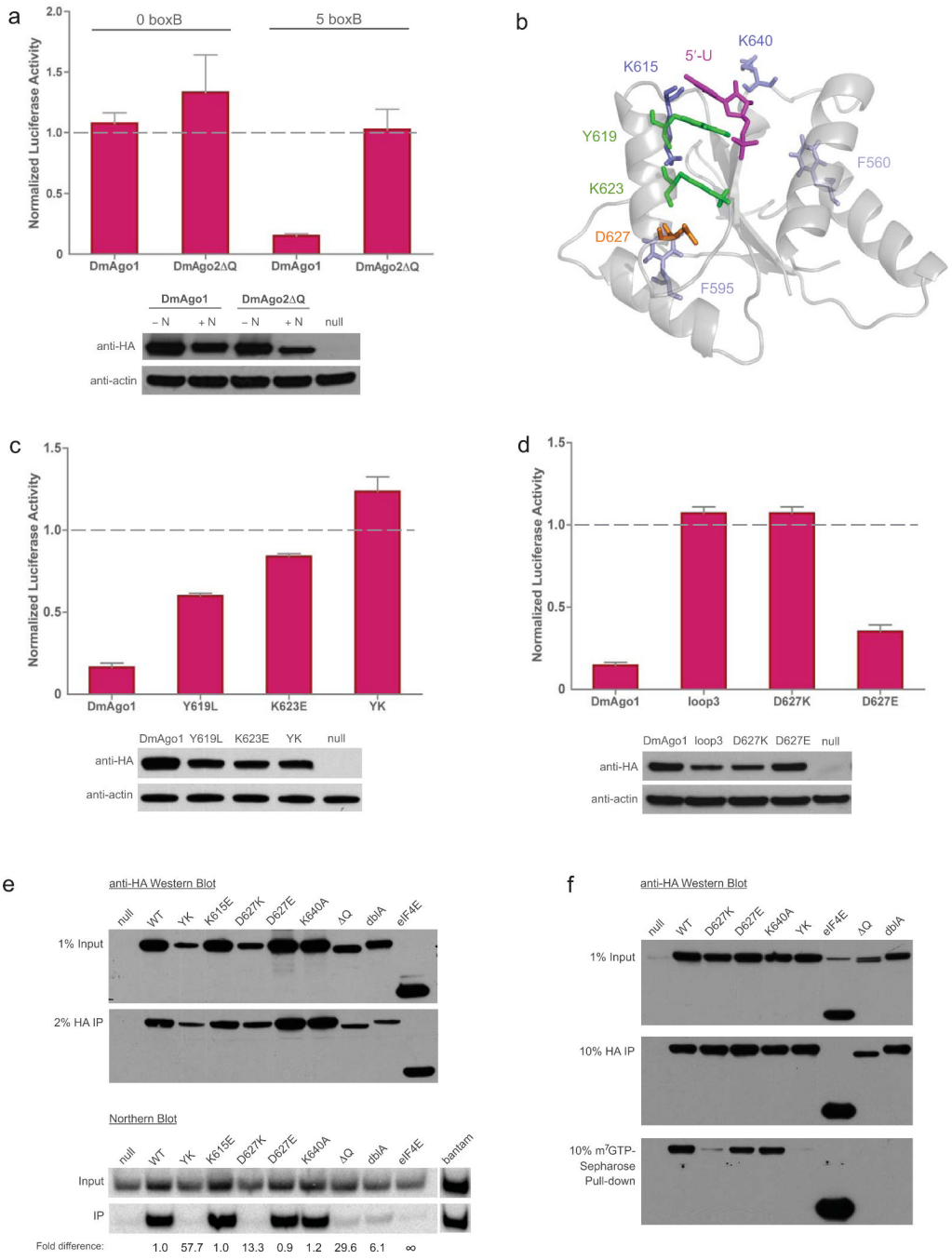

Figure 4.

Mutational analysis of Argonaute proteins in *Drosophila* S2 cells. **a, c, d,** S2 cells were transfected with a mixture of three plasmids: either the F-Luc-0BoxB or -5BoxB reporter, R-Luc transfection control and the indicated Argonaute encoding construct. HA-tagged Argonaute proteins were either fused with λN sequences or not, as indicated. For each DmAgo variant, F-Luc values were normalized to R-Luc and triplicates were averaged. Tagged (+N) values were normalized to untagged (−N) values. Western blots show expression of each tested variant. Error bars represent the standard deviation from at least three independent experiments. **a,** Repression of the FLuc reporter by DmAgo1 (but not DmAgo2ΔQ) in the tethering assay depends on the presence of 5 boxB stem loops in the reporter 3'UTR. **b,** Cartoon representation

of modeled DmAgo1 MID domain with sites of mutation and 5' nucleotide of bound miRNA indicated (5'-U in pink). Control surface residues K615 and K640 are shown in dark blue while buried residues, F560 and F595, are shown in light blue. **c,** Mutations in the 5'-end miRNA binding site of DmAgo1. **d,** Mutation of residues 627-630 in loop 3 of DmAgo1. **e, f,** S2 cells were transfected with indicated HA-tagged constructs; null contained no transfected protein. **e,** MicroRNA binding by DmAgo1 (and variants) evaluated by HA-pull-down, and subsequent northern analysis probing for *bantam* in precipitated samples. "bantam" lane contains 1 pmol of *bantam* miRNA (Dharmacon). Quantitation of northern blots indicates extent of binding differences. **f,** Binding to m^7GTP-Sepharose by HA-DmAgo1 (and variants).

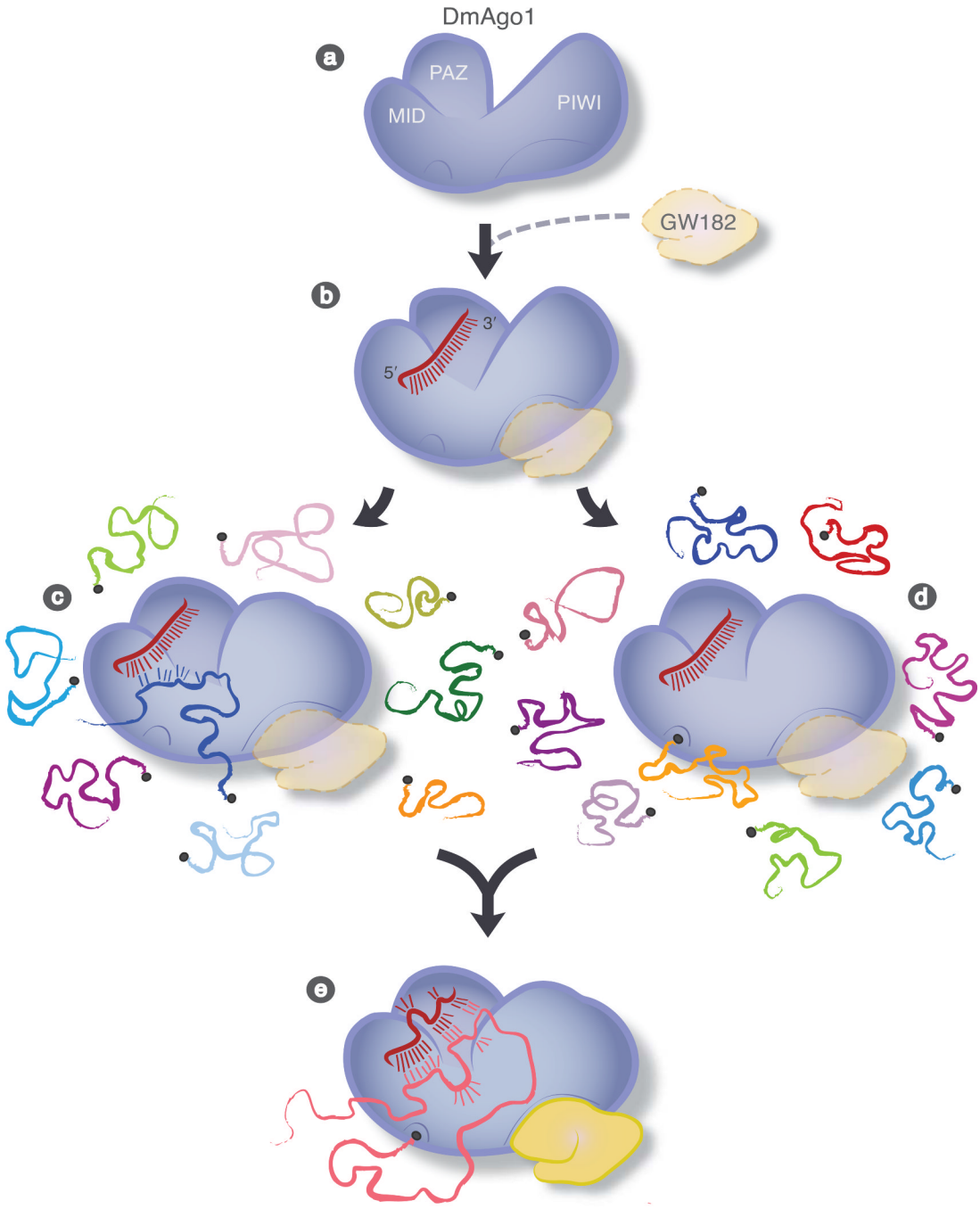

Figure 5.
Cartoon describing potential role of Argonaute allostery in promoting translational repression. **a,** Argonaute protein with various domains indicated. **b,** Initial interaction between Argonaute, miRNA and potentially GW182 (transparent) are shown. Next, miRNA-bound Argonaute either **c,** samples messages independent of cap binding or **d,** specifically scans capped messages, both pathways leading to **e,** a fully engaged Argonaute protein ready for translational repression. miRNA:target duplex, cap and GW182 are all likely bound in this final stage.